Biosensors and Bioelectronics 25 (2010) 2065–2070

Contents lists available at ScienceDirect

Biosensors and Bioelectronics

journal homepage: www.elsevier.com/locate/bios

A novel enzyme biosensor for glucose based on rhodanine derivative chemiluminescence system and mesoporous hollow silica microspheres receptor

Jinghua Yu*, Lei Ge, Ping Dai, Shenguang Ge, Shiquan Liu

School of Chemistry and Chemical Engineering, University of Jinan, Jinan 250022, PR China

ARTICLE INFO

Article history:
Received 21 October 2009
Received in revised form
29 December 2009
Accepted 1 February 2010
Available online 6 February 2010

Keywords:
Rhodanine derivative
Chemiluminescence
Enzyme biosensor
Hollow silica microspheres

ABSTRACT

In this work, hollow silica microspheres (HSMs), which have hollow interiors and nanoporous shells, were used in the immobilization of enzyme to establish a novel chemiluminescence biosensor. The immobilization behavior of enzyme in HSMs with different pore sizes has been studied. The results revealed that the pore size and the surface area of HSMs play important roles in their immobilization performance. Compared with traditional methods, this immobilization method not only provides tunable and consistent pore system and restricted microspaces for enzyme immobilization, but also exhibits a larger immobilization capacity and a higher adsorption rate. A rhodanine derivative-$KMnO_4$-HCl-H_2O_2 was used to replace traditional chemiluminescence system (luminol-horseradish peroxidase-H_2O_2) to reach the purpose of high sensitivity, simple operation and pH expansion for chemiluminescence biosensor. The linear range of this novel method is 7.72×10^{-6} to 2.54×10^{-2} mol L^{-1} ($r = 0.9994$). The detection limit is 8.0×10^{-7} mol L^{-1}. The Michaelis–Menten constant of glucose oxidase was 0.3 mmol L^{-1}. With glucose oxidase as a test enzyme, the proposed method gave an accurate and satisfactory result once applied to the determination of glucose in four different human serum samples.

1. Introduction

The immobilization of enzyme on solid inorganic supports has been a hot research area (Bickerstaff, 1997; Livage et al., 2001). Immobilized enzymes in solid supports, due to their potential to improve the stability of enzymes under extreme conditions, are quite useful for catalysis, sensor, and separation applications. Researchers have developed many approaches to immobilize enzyme, such as protein-polymer layer-by-layer assembly, crossing-linking crystals, sol–gel encapsulation and mesoporous materials adsorption (Gill et al., 1999; Jin and Brennan, 2002; Li et al., 2009; Yu et al., 2008). The microstructure of polymeric materials is normally amorphous and the catalytic activity of enzyme molecule can be deteriorated by deformation (DeLouise and Miller, 2005). Unlike silica gel, ordered mesoporous silica (OMS) materials provide tunable and consistent pore system, functionalizable surfaces, and restricted nanospaces for enzyme immobilization. OMS have become popular ever since they were synthesized and characterized by Mobil researchers in 1992 (Beck et al., 1992; Kresge et al., 1992). Recently, many research groups have immobilized enzymes on OMS and reported a significant improvement on enzyme stability, catalytic activity, products specificity, and resistance to extreme environmental conditions (Deere et al., 2002; Lee et al., 2006; Wang and Caruso, 2005). Hollow silica microspheres (HSMs) offer large internal spaces inside the shells and create a separated environment. The micro/mesopores in the shells provide a path for the substances going in and out of the interior hollows. Due to this unique structure, HSMs has not only special mechanic, acoustic, optic, electromagnetic, thermal properties, but also the immobilization property for enzyme (Han et al., 2006; Lim et al., 2002; Tartaj et al., 2001). HSMs have free silanol groups on their surfaces which can form hydrogen bonds with the free amino groups of enzymes. Besides this force, Van der Waals interaction also exists between enzyme and the surface of HSMs. Hydrophobic interactions contribute in adsorption by interaction of hydrophobic patches on the enzyme with the silicon network of HSMs. To our best knowledge, no reports about the immobilization of enzyme in HSMs have been published, its schematic representation of enzyme immobilized in HSMs with different pore size was shown in Fig. 1.

Diabetes is a worldwide health problem affecting hundreds of millions of people. Fortunately, with careful management of diet and medication, complication of diabetes can be reduced. Part of this treatment includes monitoring the glucose levels in the blood, so that proper action can be taken if its levels get too high. The glucose oxidase (GOx), which is an extremely stable enzyme and can survive wide excursions of pH, ionic strength, has made glucose measurement fast, easy, and inexpensive. The characteristics

* Corresponding author. Tel.: +86 531 82767161.
E-mail addresses: jndxgelei@gmail.com, gl-198602@163.com, 306375767@qq.com (J. Yu).

0956-5663/$ – see front matter © 2010 Elsevier B.V. All rights reserved.
doi:10.1016/j.bios.2010.02.001

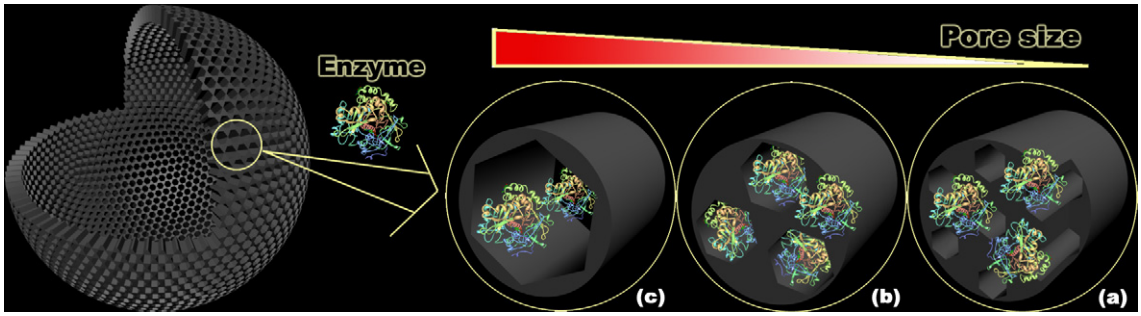

Fig. 1. Schematic representation of enzyme immobilized HSMs in different pore sizes.

of GOx in bulk solution are well documented (Bright and Gibson, 1967; Bergmeyer, 1974; Gibson et al., 1964; Rogers and Brandt, 1971). Therefore, in this work, we chose GOx as our test enzyme to establish a novel chemiluminescence biosensor.

In recent years, a number of studies have been conducted to develop new glucose monitoring methods (Fang et al., 1997; Li et al., 2008; Park et al., 2006; Zhang et al., 2005). Among them flow injection-chemiluminescence (FI-CL) biosensor is the most popular. Typical FI-CL biosensor for glucose is based on its enzymatic reaction with the GOx, producing gluconic acid and hydrogen peroxide (H_2O_2). Then the determination of glucose can be achieved via CL reaction between the enzymatic produced H_2O_2 and luminol-horseradish peroxidase (HRP) CL system (Li et al., 2008). In luminol CL system, an alkaline medium (pH 10–12) should be afforded, which limits the use of CL biosensor. In this paper, we demonstrate a novel rhodanine derivative CL system, which can be used in acid medium. Thus, the application of this rhodanine derivative CL system would expand the applicable pH range of CL biosensor. We replaced the traditional flow-though cell with a polymethyl methacrylate module and with the Y-shaped flow path drilled through it, by which the CL reactants can be injected simultaneously.

Rhodanine is a traditional chromogenic reagent (Savvin and Gur'eva, 1987). Its derivatives after substituting different groups in a rhodanine matrix also have excellent chemiluminescence and fluorescence performance which were found and studied in our lab (Yu et al., 2009; Yu et al., 2009a; Ge et al., 2010; Yu et al., 2009b; Yu et al., 2009c). To our best knowledge, no reports about monitoring of glucose by rhodanine CL system have been published. In this work, for the first time, a rhodanine derivative 3-p-nitrylphenyl-5-(4′-methyl-2′-sulfonophenylazo)rhodanine (M4NRASP) has been used in CL system to replace the traditional luminol-HRP CL system (Yu et al., 2009c). We found this derivative CL system has high sensitive CL response in the determination of H_2O_2.

In this work, the use of HSMs for enzyme immobilization was demonstrated and it was used as receptor to establish a biosensor. The adsorption capacity of HSMs with different pore sizes was compared. We found that the monitoring capacity of the biosensor was enhanced remarkably when the HSMs-enzyme receptor was combined with rhodanine derivative CL system. This novel method has a higher sensitivity, better selectivity and shorter response time, thus the goals of simplifying the experimental setup and expanding the applicable pH range of CL biosensor have been reached.

2. Material and methods

2.1. Chemicals and reagents

HSMs were synthesized as per method described below. Rhodanine derivative was obtained from our lab (Yu et al., 2009c). GOx (E.C. 1.1.3.4; Aspergillus Niger type; 146,000 U g^{-1}) was purchased from Sigma. All reagents were of analytical reagent grade or above. Oxygen-saturated phosphate buffer solution (PBS) (pH 7.4) is used in the experiments for glucose determination and Michaelis–Menten constant studies. A 1.0×10^{-2} mol L^{-1} stock glucose-PBS standard solution was obtained by dissolving 0.4954 g of glucose (Aladdin, Shanghai, China) with little doubly distilled-deionized water and then diluting to 250 mL with PBS (pH 7.4). Working glucose-PBS standard solutions was prepared by diluting of this stock standard solution with PBS (pH 7.4). A stock standard solution containing 5.0×10^{-3} mol L^{-1} M4NRASP was prepared by dissolving 0.5656 g of M4NRASP with anhydrous alcohol and then diluting to 250 mL with doubly distilled-deionized water. A working standard solution of M4NRASP was obtained by dilution of the stock standard solution with doubly distilled-deionized water. A 5.0×10^{-3} mol L^{-1} stock solution of potassium permanganate was prepared by dissolving 0.0790 g $KMnO_4$ (Aladdin, Shanghai, China) with 500 mL doubly distilled-deionized water.

2.2. Apparatus and manifold

Doubly distilled-deionized water was obtained by SYZ-550 quartz sub-boil high-purified water distiller (Jiang Su Jin Tan, Jiang Su, China). The pH measurements were performed by using a PHS-3C digital pH-meter (Shanghai Lei Ci Device Works, Shanghai, China) with a combined glass-calomel electrode. A TU-1901 two-beam UV–vis spectrophotometer was used with 1 cm quartz cell (Perkin-Elmer, America). The nitrogen sorption and pore diameters measurements were performed on Micromeritics ASAP 2020 surface area and porosity analyzer. A CS 501 super-constant temperature bath (Chongqing, China) was used to keep temperature constant. The IFFM-D flow injection CL analyzer (Xi'an Remex Electronic Instrument High-Tech Ltd., China) was equipped with an automatic injection system and a detection system. Peristaltic pumps were used to deliver all solutions and PTFE tubing (0.8 mm id) was used to connect the flow system.

2.3. Preparation of HSMs

The synthesis details of the HSMs can be found in Ref. (Liu et al., 2008). 0.10 mol Tetraethyl orthosilicate (TEOS, Alfa Aesar) and 0.06 mol octyl amine (OA, Alfa Aesar) were first mixed for 3 min with a stirring rate of 600 rpm. Then 7.50 mol doubly distilled-deionized water containing 0.01 mol hydrochloric acid (conc.) was quickly added. After further reaction of 5 min under stirring, the resulting precipitate was collected by vacuum filtration and air-dried. Then it was calcined at 550 °C for 6 h with a heating rate of 1 °C/min, and encoded as A. For the pore expansion, uncalcined samples were hydrothermally treated at 80 °C and 100 °C respectively. After being calcined, they were encoded as B and C.

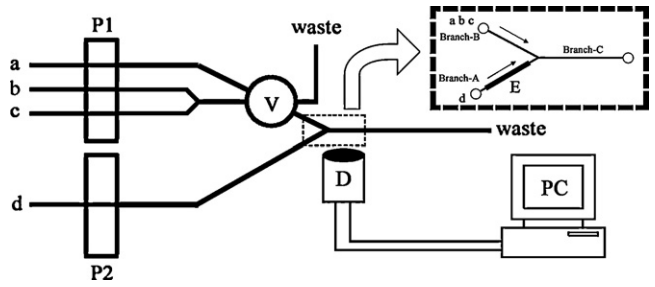

Fig. 2. Schematic diagram of the CL biosensor for the determination of glucose: (a) potassium permanganate; (b) M4NRASP; (c) HCl; (d) sample solutions (or glucose-PBS standard solution or PBS blank solution); (P1) main pump; (P2) deputy pump; (V) 6-way-valve; (D) photomultiplier; (E) glucose-sensitive receptor; (PC): personal computer.

Nitrogen sorption measurements were carried out at 77 K on Quantachrome Autosorb-1-MP automated gas adsorption system. The samples were degassed at 200 °C for 16 h. The surface areas were calculated with the Brunauer–Emmett–Teller (BET) method, using the adsorption data within the range of relative pressure P/P_0 from 0.05 to 0.15. The pore diameters were based on Barrett–Joyner–Halenda (BJH) method. The scanning electron microscopy (SEM) images were recorded on a JEOL JSM-5510 scanning electron microscope.

2.4. Enzyme immobilization

In a vessel covered to prevent evaporation, 10 mg HSMs was added to GOx solution (20 mg mL^{-1}, pH 7.4 phosphate buffer) at 4 °C under stirring for 12 h to establish the adsorption equilibrium. The amount of immobilized enzyme was calculated by subtracting the amount in the supernatant liquid after adsorption from the amount of enzyme present before adding the adsorbent by UV–vis absorption at 455 nm. Centrifugation prior to analysis was performed to avoid potential interference from scattering particles in UV–vis analysis. The UV–vis spectra of the enzyme solutions were recorded before and after the immobilization experiments to ensure that the changes in the intensity of the adsorption group (flavin group) were solely due to the change in enzyme solution concentration.

2.5. Procedure

As shown in Fig. 2, we designed a novel flow path by drilling a Y-type flow path on a polymethyl methacrylate module as receptor, through which the CL reactants were injected simultaneously. One of its branches, which was filled with HSMs-GOx, was named as Branch-A. Branch-A was plugged with glass wool at both ends. Three PTFE tubes (a–c), which were pumped by main pump though a 6-way-valve, were dipped into M4NRASP solution, potassium permanganate solution and HCl solution respectively and connected to Branch-B finally. One PTFE tube (d), which was pumped by deputy pump, was dipped into sample solution/glucose-PBS standard solution or PBS (blank solution) and connected to Branch-A finally. The Branch-C of the Y-type tube was a rotary flow path in front of detector. The deputy pump was started before the main pump to inject sample solution/glucose-PBS standard solution and PBS to protect the HSMs-GOx from being denatured by potassium permanganate solution and HCl. Then the main pump were started to inject M4NRASP solution, potassium permanganate solution and HCl to obtain the CL intensity of sample/glucose-PBS standard solution (I) and that of PBS (I_0) respectively. The concentration of glucose was quantified via the relative CL intensity (ΔI) obtained by subtracting the I_0 from I.

3. Results and discussion

3.1. Characterization of HSMs

From the SEM micrographs of sample A (Fig. 3a and b), hollows, indicated by the broken microspheres, are observed. After the hydrothermal treatment for expanding the pore size, the particle morphology keeps intact. The N_2-sorption isotherms for the three calcined samples were shown in Fig. 3c. Sample A showed an isotherm without an obvious capillary condensation, indicated that it had pores smaller than 2 nm. In contrast, samples B and C depict isotherms with quite steep capillary condensation steps, suggested that they were mesoporous. The shift of the capillary condensation step to higher relative pressures indicated that sample C had larger pore diameter than sample B. The pore size distribution curves of the three calcined samples are shown in Fig. 3d, the pore diameters of samples A, B and C are <2 nm, 7.1 nm and 11 nm, respectively. Pore expansion is evident after the hydrothermal treatment. The surface area of samples A, B and C are 1108 $m^2 g^{-1}$, 882 $m^2 g^{-1}$ and 438 $m^2 g^{-1}$, respectively. Compared with sample A, samples B and C show significant elevation of the adsorption plateau in the isotherm, indicating large increase in the pore volume of the hydrothermally treated samples. However, the pore volume of sample C is slightly smaller than that of sample B, which can be due to its more condensed network.

3.2. Adsorption performance of HSMs

The adsorption isotherm of GOx is shown in Fig. 4a. The amounts of immobilized GOx on samples A, B and C were quite different. As shown in Fig. 4a, the maximum amount of immobilized GOx was 5.5 mg (sample A/2 nm), 13.1 mg (sample B/7.1 nm) and 10.8 mg (sample C/11 nm) per 10 mg. In other paper, such as SBA-15 (Lei et al., 2004) and silicate clay mineral (Sinegani et al., 2005) had only 5 mg and 0.3 mg per 10 mg capacity of GOx immobilization respectively. This obvious difference can probably attribute to the large amount of pores in HSMs indicated in Fig. 1 and Fig. 3d. The immobilized GOx amounts in samples B and C were almost two times as many as that in sample A. Furthermore, the rates of the immobilization of GOx into samples A, B and C were also quite different.

Presumably, as sample A has a pore diameter of <2 nm while GOx is 6.75 nm long and 6.75 nm wide (PDB (Protein Data Bank) file: 1cf3), GOx could not enter the pores of sample A. Therefore, GOx loading shown in Fig. 4a is only on the external surface of sample A. To confirm the immobilization of GOx in the pores of HSMs, N_2-sorption isotherms were investigated using sample B as an example before and after GOx loading. The N_2-sorption isotherms and pore size distribution curves before and after loading GOx in sample B were shown in Fig. 4b. It is noted that the pore size distribution curve shifts to a smaller size after the loading GOx, indicating that the GOx molecules were inside the mesopores. The enzyme may get inside to the hollow interiors of samples B and C through the pores on its shell. This could further assist in utilization of the inner surface and the interiors of the HSMs and its pores. On the other hand, hollow-typed structure with pores in shell could create microflow between the space of inside and outside of the microsphere through pores, this could be very helpful for enzyme molecules to approach the inside and outside surface of the microsphere. That can explain why the adsorption rate increased sharply with increasing pore size. i.e. sample C > sample B > sample A. Moreover, we observed an intriguing experimental phenomenon: the reduction of the maximum amount of adsorbed GOx on sample C compared with that on sample B. It was probably because the surface area of sample C was reduced sharply following the increasing of its pore size. In a word, the difference of immobilized amount of GOx among three samples with different pore sizes suggests that the capacity of solid

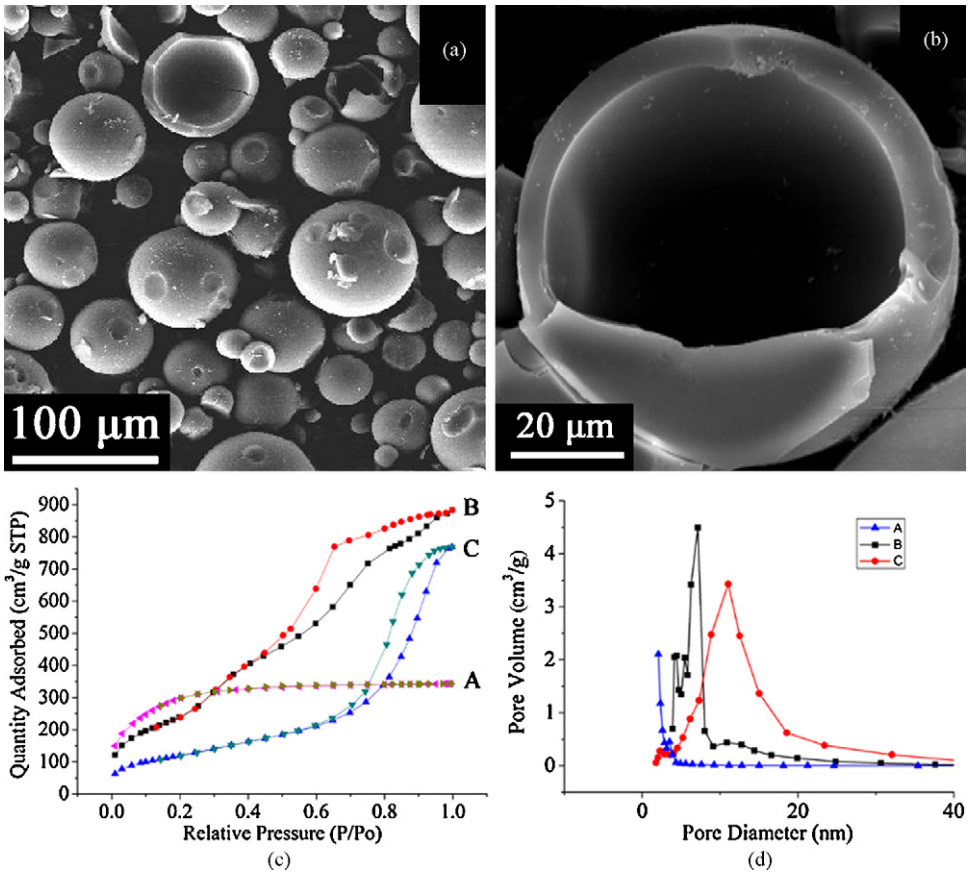

Fig. 3. Characterization of HSMs. (a) Low magnification SEM images of the HSMs; (b) high magnification SEM images of the HSMs; (c) N_2-sorption isotherms curve of samples A, B and C; (d) Pore size distribution curve of samples A, B and C.

support for GOx adsorption was not only related to the surface area of support, but also to the pore size of HSMs and the size of GOx. Based on the above observations, we chose sample B as the solid support to establish the CL biosensor below.

3.3. Stability of the proposed biosensor

The operational stability of the enzyme immobilized HSMs was investigated in the flow injection system at room temperature. Oxygen-saturated PBS (pH 7.4) was used as the carrier solution, the concentration of glucose in carrier solution was 1.0×10^{-4} mol L^{-1}, the pump rate of main pump and deputy pump was 1.4 mL min^{-1} and 1.8 mL min^{-1} respectively. The storage stability of the enzyme immobilized HSMs was investigated at 4 °C in air. Under the conditions mentioned above, this biosensor can be used for 400 continuous repeated measurements with the relative standard deviation of CL signal intensity less than 5%. After 600 continuous repeated measurements, a 30% decrease of the intensity of CL signal was observed. When the biosensor was stored in air at 4 °C for 6 weeks, it remained about 90% of its initial CL intensity.

3.4. Determination of the Michaelis–Menten constant of GOx

The Michaelis–Menten constant (K_M) of GOx, which is a characteristic constant depending on the category and the affinity to substrate of enzyme, should not be influenced by the concentra-

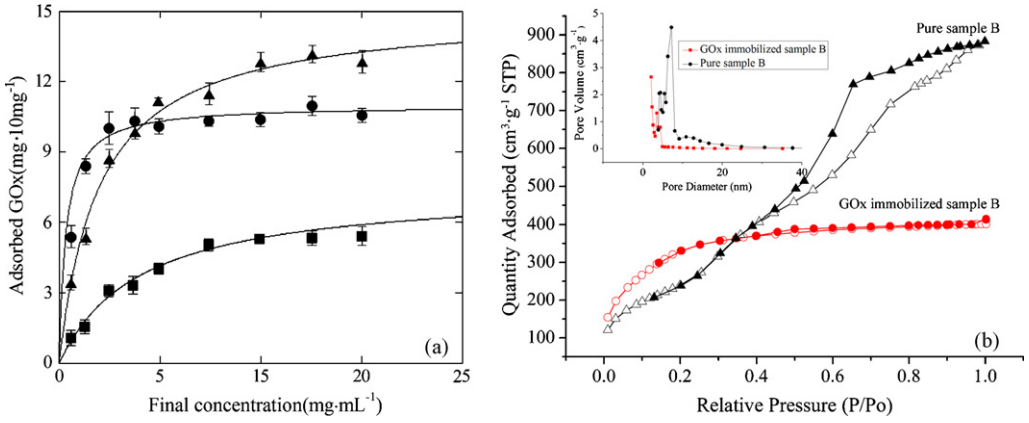

Fig. 4. Adsorption performance of HSMs. (a) The adsorption isotherm of GOx on sample A (■), sample B (▲) and sample C (●). (b) Change in nitrogen adsorption isotherms and pore size distribution before and after loading GOx in sample B.

tion of enzyme. The lower K_M is, the stronger affinity to substrate is, which indicates an improvement of the enzyme/substrate reaction; and vice versa. GOx is a double-substrate enzyme. The reaction among GOx, glucose and O_2 is a ping-pong type reaction, therefore, the Michaelis–Menten constant of GOx was calculated by the double-substrate equation as follow:

$$v = \frac{v_{lim}}{1 + \frac{K_{MG}}{[S_G]} + \frac{K_{MO}}{[S_O]}}$$

where v is the rate of reaction, v_{lim} is the limit rate of reaction measured under saturated substrate condition, $[S_G]$ is the bulk concentration of glucose, $[S_O]$ is the bulk concentration of O_2, K_{MG} is the Michaelis–Menten constant for glucose and K_{MO} is the Michaelis–Menten constant for O_2. As mentioned above, oxygen-saturated PBS (pH 7.4) was used in the experiments for Michaelis–Menten constant studies. In this receptor, the K_{MG} of GOx in HSMs was 0.3 mmol L^{-1}. This was lower than 2.9 mmol L^{-1} for GOx in sol–gel matrix (see supporting information), 30–37 mmol L^{-1} for native or free GOx (Kalisz et al., 1990; Szajani et al., 1987; Takegawa et al., 1989) and immobilized GOx in other papers (Li et al., 2009; Liu et al., 2008a; Qiu et al., 2009a; Wu et al., 2007; Yu et al., 2008), indicated that the immobilization of GOx in HSMs remarkably enhanced affinity of GOx to glucose.

3.5. Optimization of CL detection system

HCl, H_2SO_4 and NaOH were used respectively as medium to determine the effect of oxidant ($KMnO_4$, $Ce(SO_4)_2$ and $K_3[Fe(CN)_6]$) to CL. The most robust and stable CL intensity compared to negative control was obtained in $KMnO_4$–HCl system (data in supporting information). With the concentrations of HCl at the range of 0.5–3.0 mol L^{-1}, the most robust and stable CL intensity was obtained at 2.2 mol L^{-1}. The concentration of $KMnO_4$ had great effect on CL reaction. The effect of the concentration of $KMnO_4$ to CL intensity was investigated in the range of 2.5×10^{-4} to 6.0×10^{-4} mol L^{-1}. The results showed that the optimal concentration of $KMnO_4$ was 4.0×10^{-4} mol L^{-1}. The effect of M4NRASP concentration was investigated in the range 0.8×10^{-5} to 5.0×10^{-5} mol L^{-1}. The results showed that the maximal CL emission peak was obtained when the concentration of M4NRASP was 1.6×10^{-5} mol L^{-1}. Therefore, 1.6×10^{-5} mol L^{-1} M4NRASP was chosen for further study. Pump rates is a key factor for the flow biosensor. It was found that the lower pump rates were unfavorable for sensitivity because the $KMnO_4$-HCl-M4NRASP-H_2O_2 CL reaction was a fast process, and higher pump rates could cause a smaller contact time which result in an inadequate enzymatic reaction. Therefore, pump rates were optimized at the range of 1.2–3.6 mL min^{-1}. Finally, 1.4 mL min^{-1} and 1.8 mL min^{-1} was selected as both main pump's and deputy pump's optimal rate at which the relative CL intensity was robust and stable.

Table 1
Tolerance folds of coexisting substances.

Tolerance folds	Coexisting substances
≥1000	K^+, Na^+, Mg^{2+}, Cl^-, Ca^{2+}, Zn^{2+}, threonine, methionine, valine, isoleucine, lactic acid
≥500	Fe^{3+}, tryptophan, lysine, leucine
≥100	Histidine, arginine. ascorbic acid

3.6. Performance of the biosensor for glucose

Under the optimal conditions, the calibration graph was linear over the range of 7.72×10^{-6} to 2.54×10^{-2} mol L^{-1}. The linear regression equation was $\Delta I = 1553.97 + 3593.62c$ (c: $\times 10^{-4}$ mol L^{-1}) ($r = 0.9994$) (where ΔI was the relative CL intensity and c was the concentration of glucose). The relative standard deviation of this method was below 2.7% in 11 repeated measurements. The detection limit was 8.0×10^{-7} mol L^{-1}.

The linear range demonstrated in this paper was much wider than the ranges of 1.0×10^{-4} to 1.1×10^{-3} mol L^{-1} for GOx immobilized on edge plane of highly oriented pyrolytic graphite (Wang et al., 2006), 1.2×10^{-5} to 3.8×10^{-3} mol L^{-1} for GOx immobilized on multiwalled carbon nanotubes-ferrocene/chitosan-modified electrode (Qiu et al., 2009a), 1.0×10^{-5} to 1.0×10^{-3} mol L^{-1} for soluble enzyme (Economou et al., 2006), 5.0×10^{-4} to 1.6×10^{-2} mol L^{-1} based on (poly(allylamine hydrochloride/CdTe)$_x$(poly(allylamine hydrochloride/sodium polystyrenesulfonate)$_3$ (poly(allylamine hydrochloride/GOx)$_y$ multilayer (Li et al., 2009). The detection limit of 8.0×10^{-7} mol L^{-1} was lower than 1.0×10^{-4} mol L^{-1} based on GOx/controlled-pore glass receptor (Lv et al., 2003), 4.0×10^{-6} mol L^{-1} for soluble enzyme (Panoutsou and Economou, 2005), 1.9×10^{-6} mol L^{-1} based on Nafion/GOx-Au nanoparticles/glassy carbon electrode (Qiu et al., 2009), 1.0×10^{-6} mol L^{-1} based on Nafion/Pt/CMK-3-GOx-gelatin/glassy carbon electrode (Yu et al., 2008). Therefore, the immobilization of GOx in HSMs greatly widened the linear range and reduced the detection limit.

3.7. Effect of coexisting substances

The effects of various interfering species, which may accompany glucose in human serum, were also studied. All species tested were tolerated at reasonably high concentrations, showing the high selectivity of the proposed method. It is worth to mention that the

Table 2
Determination results of glucose in real samples.

Sample	Glucose concentration ($\times 10^{-3}$ mol L^{-1})				
	Proposed sensor				YSI 2300 glucose analyzer Found* ± S.D.
	Added	Found* ± S.D.	R.S.D. %	Recovery %	
Sample-1	–	2.64 ± 0.07	2.7	–	2.55 ± 0.3
	2.00	4.59 ± 0.06	1.3	97.4	4.70 ± 0.2
Sample-2	–	2.95 ± 0.08	2.7	–	2.78 ± 0.3
	2.00	5.03 ± 0.06	1.2	104.1	4.71 ± 0.1
Sample-3	–	4.47 ± 0.05	1.1	–	4.57 ± 0.1
	2.00	6.44 ± 0.13	2.0	98.3	6.49 ± 0.3
Sample-4	–	5.89 ± 0.07	1.2	–	5.68 ± 0.3
	2.00	7.88 ± 0.09	1.1	99.6	7.72 ± 0.2

* Average of 11 measurements.

influence of ascorbic acid at its physiologic normal level on the biosensor response to glucose was acceptable. The maximum tolerable concentrations of coexisting substances are shown in Table 1, where the tolerance fold was defined as the maximum concentration of coexisting substances that produced a difference between positive and negative controls.

3.8. Application to real samples

To investigate the feasibility of the sensing system for analysis of glucose in biological samples, glucose concentration in human serum was examined. Four serum samples obtained from hospitalized diabetic patients were collected by Shandong Qi Lu Hospital and were analyzed. These samples were diluted 50 times by doubly distilled-deionized water to obtain testing sample solutions. All samples were analyzed by the proposed method as well as by a Yellow Springs Instruments (YSI) 2300 glucose analyzer. Results obtained with the proposed method were compared statistically with those obtained with the automated standard colorimetric technique (Table 2).

4. Conclusions

In this work, a novel glucose-sensitive receptor assembled via immobilized enzyme in HSMs was combined with M4NRASP CL system to establish a biosensor for glucose. The immobilization behavior of GOx in HSMs with different pore sizes has been studied. It is revealed that the pore size and the surface area of the HSMs play important roles in the immobilization of enzymes. The immobilization of enzyme in the HSMs was found to be steady and have a long life time. M4NRASP, a rhodanine derivative was used and the $KMnO_4$-HCl-M4NRASP-H_2O_2 CL system was proved to be very sensitive to H_2O_2. It is of great importance for widening the application field of rhodanine derivatives as CL reagent and pH expansion for CL biosensor. The biosensor was satisfactory when applied to the determination of glucose in human serum. Quantitative detection of glucose ranging from 7.72×10^{-6} to 2.54×10^{-2} mol L^{-1} with a detection limit of 8.0×10^{-7} mol L^{-1} was achieved. The relatively lower detection limit, wider detection range, simpler determination procedure and higher stability make this CL biosensor method a power tool for glucose detection compared to traditional methods.

Acknowledgement

This work was financially supported by National Natural Science Foundation of People's Republic of China (No. 50972050); Natural Science Research Foundation of Shandong Province, China (No. Y2007B07); Postgraduate Innovation Program of Shandong Province (SDYY08030) and National High Technology Research and Development Program of China (863 Program, No. 2007AA10Z430).

Appendix A. Supplementary data

Supplementary data associated with this article can be found, in the online version, at doi:10.1016/j.bios.2010.02.001.

References

Beck, J.S., Vartuli, J.C., Roth, W.J., Leonowicz, M.E., Kresge, C.T., Schmitt, K.D., Chu, C.T.W., Olson, H.D., Sheppard, E.W., 1992. J. Am. Chem. Soc. 114, 10834–10843.
Bergmeyer, Y., 1974. Methods of Enzymatic Analysis, 2nd ed. Allied Press, New York.
Bickerstaff, G.F., 1997. Immbilization of Enzymes and Cells. Humana Press, Totowa, NJ.
Bright, H.J., Gibson, Q.H., 1967. J. Biol. Chem. 242, 994–1003.
Deere, J., Magner, E., Wall, J.G., Hodnett, B.K., 2002. J. Phys. Chem. B 106, 7340–7347.
DeLouise, L.A., Miller, B.L., 2005. Anal. Chem. 77, 1950–1956.
Economou, A., Panoutsou, P., Themelis, D.G., 2006. Anal. Chim. Acta 572, 140–147.
Fang, Q., Shi, X.T., Sun, Y.Q., Fang, Z.L., 1997. Anal. Chem. 69, 3570–3577.
Ge, S.G., Dai, P., Yu, J.H., Zhu, Y.N., Huang, J.D., Zhang, C.C., Ge, L., Wan, F.W., 2010. Intern. J. Environ. Anal. Chem., doi:10.1080/03067310903026653.
Gibson, Q.H., Swoboda, B.E.P., Massey, V., 1964. J. Biol. Chem. 239, 3927–3934.
Gill, I., Pastor, E., Ballesteros, A., 1999. J. Am. Chem. Soc. 121, 9487–9496.
Han, M., Zhang, W.L., Gao, C.L., Liang, Y.Y., Xu, Z., Zhu, J.M., He, J.H., 2006. Carbon 44, 211–215.
Jin, W., Brennan, J.D., 2002. Anal. Chim. Acta 461, 1–36.
Kalisz, H.M., Hecht, H.J., Schomburg, D., Schmid, R.D., 1990. J. Mol. Biol. 213, 207–209.
Kresge, C.T., Leonowicz, M.E., Roth, W.J., Vartuli, J.C., Beck, J.S., 1992. Nature 359, 710–712.
Lee, C.H., Mou, C.Y., Ke, S.C., Lin, T.S., 2006. Mol. Phys. 104, 1635–1641.
Lei, J., Fan, J., Yu, C.Z., Zhang, L.Y., Jiang, S.Y., Tu, B., Zhao, D.Y., 2004. Microporous Mesoporous Mater. 73, 121–128.
Li, B.X., Lan, D., Zhang, Z.J., 2008. Anal. Biochem. 374, 64–70.
Li, X.Y., Zhou, Y.L., Zheng, Z.Z., Yue, X.L., Dai, Z.F., Liu, S.Q., Tang, Z.Y., 2009. Langmuir 25, 6580–6586.
Lim, T.J., Smith, B., McDowell, D.L., 2002. Acta Mater. 50, 2867–2879.
Liu, S.Q., Rao, J.C., Sui, X.Y., Cool, P., Vansant, E.F., Tendeloo, G.V., Cheng, X., 2008. J. Non-Cryst. Solids 354, 826–830.
Liu, Y.G., Feng, X.M., Shen, J.M., Zhu, J.J., Hou, W.H., 2008a. J. Phys. Chem. B 112, 9237–9242.
Livage, J., Coradin, T., Roux, C., 2001. J. Phys.: Condens. Matter. 13, R673–R692.
Lv, Y., Zhang, Z.J., Chen, F.N., 2003. Talanta 59, 571–576.
Panoutsou, P., Economou, A., 2005. Talanta 67, 603–609.
Park, S., Boo, H., Chung, T.D., 2006. Anal. Chim. Acta 556, 46–57.
Qiu, H.J., Xue, L.Y., Ji, G.L., Zhou, G.P., Huang, X.R., Qu, Y.B., Gao, P.J., 2009. Biosens. Bioelectron. 24, 3014–3018.
Qiu, J.D., Zhou, W.M., Guo, J., Wang, R., Liang, R.P., 2009a. Anal. Biochem. 385, 264–269.
Rogers, M.J., Brandt, K.G., 1971. Biochemistry 10, 4624–4630.
Savvin, S.B., Gur'eva, R.F., 1987. Talanta 34, 87–101.
Sinegani, A.A.S., Emtiazi, G., Shariatmadari, H., 2005. J. Colloid Interface Sci. 290, 39–44.
Szajani, B., Molnar, A., Klamar, G., Kalman, M., 1987. Appl. Biochem. Biotechnol. 14, 37–47.
Takegawa, K., Fujiwara, K., Iwahara, S., Yamamoto, K., Tochikura, T., 1989. Biochem. Cell Biol. 67, 460–464.
Tartaj, P., Gonzalez-Carreno, T., Serna, C.J., 2001. J. Adv. Mater. 13, 1620–1624.
Wang, Y., Caruso, F., 2005. Chem. Mater. 17, 953.
Wang, G., Thai, N.M., Yau, S.T., 2006. Electrochem. Commun. 8, 987–992.
Wu, B.Y., Hou, S.H., Yin, F., Li, J., Zhao, Z.X., Huang, J.D., Chen, Q., 2007. Biosens. Bioelectron. 22, 838–844.
Yu, J.J., Yu, D.L., Zhao, T., Zeng, B.Z., 2008. Talanta 74, 1586–1591.
Yu, J.H., Dai, P., Ge, S.G., Zhang, L.N., Tan, Y., Li, B., 2009. Spectrosc. Lett. 42, 42–48.
Yu, J.H., Dai, P., Ge, S.G., Zhu, Y.N., Zhang, L.N., Cheng, X.L., 2009a. Spectrochim. Acta Part A 72, 17–21.
Yu, J.H., Wan, F.W., Dai, P., Ge, S.G., Bo, L., Huang, J.D., 2009b. Anal. Lett. 42, 746–757.
Yu, J.H., Dai, P., Wan, F.W., Li, B., Ge, S.G., 2009c. J. Sep. Sci. 32, 2170–2179.
Zhang, Z.Y., Zhang, S.C., Zhang, X.R., 2005. Anal. Chim. Acta 541, 37–46.